ON THE USE OF A BI-DIMENSIONAL MODEL TO INVESTIGATE A VIAL FREEZE-DRYING PROCESS

Salvatore A. Velardi, Antonello A. Barresi

Dipartimento di Scienza dei Materiali e Ingegneria Chimica, Politecnico di Torino.
Corso Duca degli Abruzzi 24, 10129 Torino, Italy

This paper is focused on the development and evaluation of a bi-dimensional model to investigate a vial freeze-drying process. The equations of the model define a moving boundary problem (Stefan problem) and the mathematical artifice of the axial immobilisation of the moving interface is used to avoid a spatial grid evolving with time, as the position of the sublimating interface is not fixed. Results obtained through mathematical simulation of the process are validated against experimental results, thus evidencing the effectiveness of the proposed approach. A "double axial-radial immobilisation" of the moving front is finally proposed in order to enable the model to predict the formation of the ice core occurring when the radial velocity of the moving front becomes higher than the axial one, due to the relative weight of the heat contribution from the vial sides and from the top and bottom of the vial.

1. INTRODUCTION

Freeze-drying is a process used to remove water from a frozen product by means of sublimation of the ice at low pressure. This process has been extensively applied in food and pharmaceuticals processing as the low operating temperatures avoid impairing the final quality of heat sensitive products. In this paper we will focus on pharmaceuticals freeze-drying: glass vials generally contain the product, and are placed over a shelf in the drying chamber: vials for freeze-drying have generally a special design, with a very flat bottom, to favour heat transfer from shelf. After the initial freezing, the pressure in the chamber is reduced at the target value, typically 5-30 Pa, and the product is heated through the shelf as the sublimation is an endothermic process (primary drying). Finally, when all the ice has been removed, the shelf temperature is increased (secondary drying) to remove the bound water, thus reaching the target level of residual moisture in the product. The operating conditions (shelf temperature and chamber pressure) have to be carefully selected in order to preserve product quality at the end of the drying. In particular, product temperature has to remain below a value that depends on the characteristics of the product itself and on its formulation. Currently, the development of freeze-drying recipes is done largely on a trial and error basis, a slow and expensive procedure that often does not yield fully optimized freeze-drying cycles. However, there is increasing interest in reducing cycle development time by using computer simulations either to help finding a fully optimised freeze-drying recipe (see for example Velardi and Barresi, 2008) and to obtain quickly the design space (Giordano et al., 2011) or to allow reliable process transfer and scale up (Fissore et al., 2010): in fact, mathematical modelling could satisfactorily predict the dynamic behaviour of the various stages of the freeze-drying process under different operational policies (Liapis et al., 1996) and can be used also for equipment design and optimisation (Barresi et al., 2010).
Simple mathematical models of the vials neglecting radial gradients of temperature and composition (ice fraction) were proposed in the past (see Velardi and Barresi (2008) and the papers quoted therein) and successfully used to design soft-sensors for process monitoring (Velardi et al., 2009 and 2010) as well as model-based tools for in-line control (Pisano et al., 2010); they were also used in multi-scale modelling of the process, including both the product in the containers and the drying chamber, eventually coupled with Computational Fluid Dynamics (CFD) codes (Rasetto et al., 2010). Detailed multi-dimensional models could be much more

useful for *in silico* investigation of the process and off-line optimization, due to the time required by the calculations. Tang et al. (1986) firstly presented a bi-dimensional axisymmetric model to investigate vial freeze-drying of pharmaceutical aqueous solutions, without numerical results. This approach was proposed also by Liapis and Bruttini (1995) to prove that the temperature of the interface of sublimation cannot be constant when radiative flux at the vial side is taken into account, and that the free surface at the edge of the vial is always curved downward.

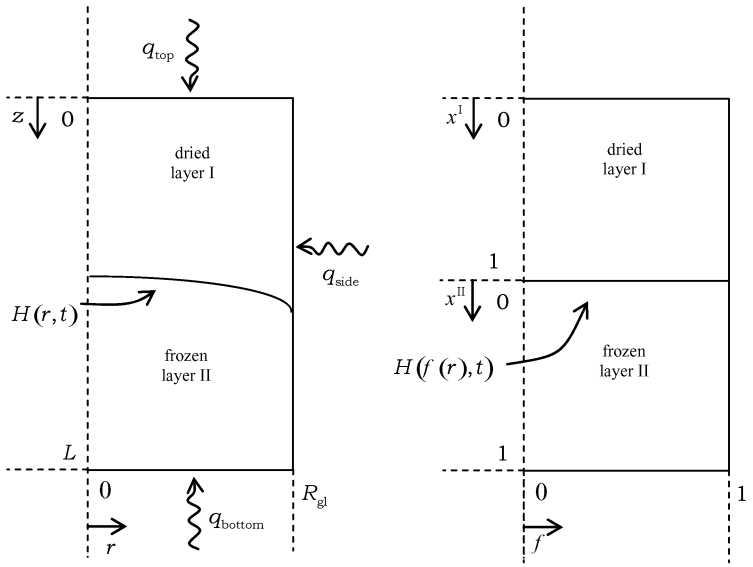

Fig. 1: Schematic of the vial geometry. Left hand side: dimensional coordinate system. Right hand side: non-dimensional coordinate system, after the axial immobilisation of the moving interface.

First numerical results produced by a bi-dimensional model were presented by Mascarenhas et al. (1997), where a finite-element formulation was used in order to solve the model: an Arbitrary Lagrangian-Eulerian description is used, treating the finite-element mesh as a reference frame that may be moving with an arbitrary velocity. Mass and heat balances are the same proposed by Liapis and Bruttini (1995). A finite-element formulation was also used by Lombraña et al. (1997) to solve the bi-dimensional model of vial freeze-drying of special food.
According to Sheehan and Liapis (1998) the formulation adopted by Mascarenhas et al. (1997) and by Lombraña et al. (1997) has major problems because: it fails to describe the dynamic behaviour of the primary drying stage in a vial when the moving interface between the dried and frozen layer does not extend along the whole length of the diameter of the vial; it cannot provide the proper drying time and drying rate for the secondary drying stage because it cannot account in the primary drying stage for the removal of all the ice as said before; and finally it cannot describe properly the dynamic behaviour of the geometric shape and position of the moving interface because the water vapour mass flux is considered to be time invariant when the position of the moving interface is located between mesh points of the grid. However these concerns are more related to the way the problem is treated from a numerical point of view. Thus, Sheehan and Liapis (1998) solved the same equations, but with a different numerical method based on the orthogonal collocations. Numerical simulations showed that when there is no heat input from the vial sides, no physical stimulus exists as well to induce radial effects, and the geometry of the moving interface is flat: in this case the problem solution coincides with that given by Sadikoglu and Liapis (1997) for the one-dimensional case. This situation is representative for the vast majority of the vials undergoing freeze-drying, that is the vials located at the centre of the shelf, if the axial heat conduction in the wall of the vials is neglected. However, some vials suffer for radiative effects due to their position close to the chamber wall and/or to the edge of the metal tray or other containing devices, when used. Simulations showed

that these vials dry faster and thus should be taken into account when looking for the optimal operating conditions. However, the strong reduction of the drying time seems to be the main effect of radiation since, although a curvilinear shape is obtained for the sublimation interface of the cornel vials, the difference between the position of the interface at the centre and at the side of the vial is less than 1% of the total thickness of the product.
In the following, a detailed bi-dimensional model of the process will be presented. In order to avoid a spatial grid evolving with time, as the position of the sublimating interface is not fixed, beside the well known mathematical artifice of the axial immobilisation of the moving interface, a "double axial-radial immobilisation" of the moving front is proposed: it enables the model to predict the formation of the ice core occurring when the radial velocity of the moving front becomes higher than the axial one, due to the relative weight of the heat contribution from the vial sides and from the top and bottom of the vial.

2. MATHEMATICAL MODELING

Starting from the equations proposed by Liapis and Bruttini (1995), Mascarenhas et al. (1997), and Sheehan and Liapis (1998), a numerical code for the bi-dimensional unsteady-state simulation of the primary drying stage of freeze-drying in vial has been set up. A schematic of the vial, assumed to be cylindrical, is shown in Figure 1. Only half a vial is depicted because of the assumption of axial-symmetry. Two distinct regions can be pointed out: region I is the dried layer, which extends from the top of the vial to the sublimating interface. In layer I water has been mostly removed by sublimation and partially by desorption, leaving a porous matrix through which water vapour is transported by diffusion and convection. Region II is constituted by the frozen product. During the primary drying phase the moving interface, here denoted with the function $H(r, t)$, recedes due to sublimation. If a heat input q_{side} is provided in radial direction, as it occurs when radiation from the chamber to the vial sides is present, the shape of the interface becomes curved. It should be pointed out that normally radiation is not evenly distributed at the vial sidewall and only a more complex tri-dimensional model could take into account the different contribution at any angular position. Anyway in previous work the simplified assumption was made that the radiative contribution is the same along the perimeter of the vial, and the presence of the wall favour a radial redistribution. It must be considered that another source of radial heat is that supplied through the wall from the shelf, and it may be comparable with the radiating one. Thus as a first approach the assumption of axial-symmetry is considered valid. When the interface has reached the bottom of the vial in correspondence of the maximum radial position, it begins to narrow and finally if degenerates into a point at the bottom centre. When the frozen layer II has disappeared only secondary drying takes place, which continues until the residual water content decreases to the desired value.

Table 1: Equations of the bi-dimensional model.

Energy balance for the dried layer I	$\rho_{\text{Ie}} c_{P,\text{Ie}} \dfrac{\partial T_{\text{I}}}{\partial t} = -c_{P,G}\mathbf{N}_{\mathbf{tot}} \cdot \nabla T_{\text{I}} + \nabla \cdot \left(k_{\text{Ie}} \nabla T_{\text{I}}\right) + \Delta H_{\text{v}} \dfrac{\partial \rho_{\text{sw}}}{\partial t} = 0,\ 0 < z < H\left(r,t\right)$
Energy balance for the frozen layer II	$\rho_{\text{II}} c_{P,\text{II}} \dfrac{\partial T_{\text{II}}}{\partial t} = \nabla \cdot \left(k_{\text{II}} \nabla T_{\text{II}}\right),\ H\left(r,t\right) < z < L$
Continuity equation for water vapour	$\varepsilon_P \dfrac{\partial \rho_{\text{w}}}{\partial t} = -\nabla \cdot \mathbf{N}_{\mathbf{w}} - \dfrac{\partial \rho_{\text{sw}}}{\partial t},\ 0 < z < H\left(t\right)$
Continuity equation for the inert gas	$\varepsilon_P \dfrac{\partial \rho_{\text{in}}}{\partial t} = -\nabla \cdot \mathbf{N}_{\mathbf{in}},\ 0 < z < H\left(t\right)$
Mass balance across the interface	$\mathbf{N}_{\mathbf{w}}\big\|_{z=H(r,t)} = -\mathbf{v}\rho_{\text{II}} + \mathbf{v}\rho_{\text{Ie}}$
Energy balance across the interface	$\mathbf{q}_{\mathbf{II}}\big\|_{z=H(r,t)} - \mathbf{q}_{\mathbf{I}}\big\|_{z=H(r,t)} - \mathbf{N}_{\mathbf{w}}\big\|_{z=H(r,t)}\left(c_{P,G}T_{\text{i}} + \Delta H_s\right) - \mathbf{v}\left(\rho_{\text{II}} c_{P,\text{II}} T_{\text{i}} - \rho_{\text{Ie}} c_{P,\text{Ie}} T_{\text{i}}\right) = 0$

The other main assumptions made in developing the model are the followings:

- Thermal equilibrium between the gas flowing through the dried layer and the porous solid: at any position the gas temperature is equal to the dried material temperature. Under this assumption a pseudo-homogeneous energy balance can be written for the system gas-dried layer, in which effective parameters are used.
- The moving boundary is assumed to be a mathematical surface, in which no accumulation of energy and mass is allowed and water vapour and frozen water are in thermodynamic equilibrium.
- The frozen region is homogeneous and contains a negligible portion of dissolved gases.
- The binary mixture of water vapour and inert gas flowing through the dried layer obeys to the ideal gas law.
- q_{side} is assumed uniform and independent of the z coordinate.

Table 2: List of symbols

c_P	specific heat at constant pressure, J kg^{-1}K^{-1}	L	total thickness of the product, m
f^i	generic function in spatial domain i	$\mathbf{N}$	mass flux, kg m^{-2}s^{-1}
$\dot{f}^i, \ddot{f}^i$	first and second derivatives of the generic function in spatial domain i	$\mathbf{q}$	heat flux, J m^{-2}s^{-1}
		r	radial coordinate, m
F	view factor for radiative heat transfer	R_{gl}	vial internal radium, m
h_1, h_2	functions used in the procedure of double axial-radial immobilisation, m	$R^*(z,t)$	front position in the procedure of double axial-radial immobilisation, m
h_v	heat transfer coefficient at vial bottom, J m^{-2}s^{-1}K^{-1}	t	time, s
$H(r,t)$	moving front position, m	T	temperature, K
ΔH_s	enthalpy of sublimation, J kg^{-1}	T_i	moving front temperature, K
ΔH_v	enthalpy of desorption, J kg^{-1}	$\mathbf{v}$	moving front velocity, m s^{-1}
k	thermal conductivity, J m s^{-1}K^{-1}	z	axial coordinate, m

Greek letters		**Subscripts and superscripts**	
δ_b	vial bottom glass thickness, m	I	layer I, dried layer
δ_s	vial side glass thickness, m	II	layer II, frozen layer
ε	emissivity	e	effective
ε_P	porosity of the dried layer	G	gas
λ_{gl}	thermal conductivity of the vial glass, J m^{-1}s^{-1}K^{-1}	gl	vial glass
ξ	non-dimensional axial-coordinate	in	inert gas
ρ	mass density, kg m^{-3}	side	vial sidewall
ρ_{sw}	bound water mass concentration, kg m^{-3}	top	vial top
σ	Boltzmann constant, J m^{-2}s^{-1}K^{-4}	tot	total (inert and water)
ϕ	non-dimensional radial coordinate	w	water vapour
		wall	freeze-drier chamber wall

The equations of the model describe the time and spatial evolution of the temperature of the dried layer, T_I, and of the frozen product, T_{II}, of the water vapour and inert gas mass concentration in the dried porous region, ρ_w and ρ_{in} respectively, and of the residual sorbed water mass concentration, ρ_{sw}; here ρ_{sw} is defined as the mass of sorbed water per volume of porous dried material. Heat is transferred through the frozen mass by conduction and through the dried layer by convection and conduction. Indeed, the terms involving ρ_{sw} could be neglected during the primary drying phase without introducing significantly errors in the model prediction, as remarked by Sadikoglu and Liapis (1997). Model equations are summarised in Table 1, while the list of the symbols used is shown in Table 2. The equations are written on a mass basis and adopting a vectorial notation. The material and

the energy balance across the moving front allows to describe the velocity **v** and the temperature T_i of the sublimating interface. The velocity vector has been determined considering that the interface recedes with a velocity due to the mass of water that leaves the front, which is equal to the difference between the frozen mass that disappears and the dried mass that originates in the process. The time evolution of the moving interface can be determined from the mass balance at the moving interface, after decomposition of **v** along the axial and radial directions. The following equation is obtained:

$$\frac{\partial H}{\partial t} = -\frac{1}{\rho_{\mathrm{II}} - \rho_{\mathrm{Ie}}}\left(N_{\mathrm{w},z}\Big|_{z=H(r,t)} - N_{\mathrm{w},r}\Big|_{z=H(r,t)} \frac{\partial H}{\partial r} \right) \tag{1}$$

Non-isobaric mass transfer in the porous medium is modelled considering Newtonian flow, Knudsen diffusion and mutual diffusion all occurring simultaneously. Thus, the "dusty gas model" equations were adopted in order to express the mass fluxes of water vapour, $\mathbf{N_w}$, and inert gas, $\mathbf{N_{in}}$ (Mason et al., 1967; Kast and Hohenthanner, 2000).

The heat for sublimation and desorption is provided from the heating plates placed above and below the vial, and radiation from the chamber walls to the vial sides is also considered. The heat supplied defines the interaction of the vial with the chamber environment, and is simulated through boundary conditions variable with time. The boundary conditions for energy transfer at the top ($z = 0$) and at the bottom of the vial ($z = L$) are the followings:

$$\begin{aligned} &z = 0, \quad \forall r \quad -k_{\mathrm{I,e}} \frac{\partial T_{\mathrm{I}}}{\partial z}\Big|_{z=0} = q_{\mathrm{top}} = \varepsilon\sigma F_{\mathrm{top}} \left(T_{\mathrm{shelf}}^4(t) - T_{\mathrm{I}}^4\Big|_{z=0} \right) \\ &z = L, \quad \forall r \quad k_{\mathrm{II}} \frac{\partial T_{\mathrm{II}}}{\partial z}\Big|_{z=L} = \left(\frac{1}{h_{\mathrm{v}}} + \frac{\delta_{\mathrm{b}}}{\lambda_{\mathrm{gl}}} \right)^{-1} \left(T_{\mathrm{shelf}}(t) - T_{\mathrm{II}}\Big|_{z=L} \right) \end{aligned} \tag{2}$$

Heat transfer at the vial sides is defined by the boundary condition given by eq. (3):

$$t > 0, \quad \forall z, \; r = R_{\mathrm{gl}} \quad k_j \frac{\partial T_j}{\partial r}\Big|_{r=R_{\mathrm{gl}}} = q_{\mathrm{side}} \qquad (j = \mathrm{I}, \mathrm{II}) \tag{3}$$

where q_{side} must account for the different contributions (including conduction along the vial wall). If only the contribution by radiation is relevant, q_{side} can be written as:

$$q_{\mathrm{side}} = \varepsilon\sigma F_{\mathrm{side}} \left(T_{\mathrm{wall}}^4(t) - T_{\mathrm{gl}}^4\Big|_{r=R_{\mathrm{gl}}+\delta_s} \right) \tag{4}$$

Considering a linear temperature profile along r in the glass, q_{side} can be also expressed as a function of the temperature driving force between the dried layer and the external side of the vial, allowing to eliminate the unknown temperature $T_{\mathrm{gl}}\Big|_{r=R_{\mathrm{gl}}+\delta_s}$ from equation (4):

$$q_{\mathrm{side}} = \frac{\lambda_{\mathrm{gl}}}{\left(R_{\mathrm{gl}} + \delta_{\mathrm{s}}\right) \ln \frac{R_{\mathrm{gl}} + \delta_{\mathrm{s}}}{R_{\mathrm{gl}}}} \left(T_{\mathrm{gl}}\Big|_{r=R_{\mathrm{gl}}+\delta_s} - T_j\Big|_{r=R_{\mathrm{gl}}} \right) \quad (j = \mathrm{I}, \mathrm{II}) \tag{5}$$

View factors for batch of vials arranged in square and hexagonal arrays are found in the paper by Sheehan and Liapis (1998) and can be calculated from geometrical considerations (Lienhard and Lienhard, 2004). When ice disappears the secondary drying stage begins, no moving interface exists anymore, and the model reduces to the energy balance for the dried layer I and to the continuity equations for water vapour and for the inert gas.

3. NUMERICAL SOLUTION OF THE MODEL

The equations of the model define a moving boundary problem, also known as Stefan problem. The resolution of the system of equations would imply the utilisation of a spatial grid evolving with time, as the position of the sublimating interface is not fixed. In order to overcome this problem a mathematical artifice can be used, consisting in the axial immobilisation of the moving interface. Following the procedure suggested by Sheehan and Liapis (1998), the immobilisation can be performed introducing two non-dimensional axial variables, $\xi^{I}, \xi^{II} \in [0,1]$, thus obtaining a spatial grid fixed in time. The axial variable ξ^{I} describes the domain of the dried layer I, while ξ^{II} defines the domain of the frozen layer II. The radial variable *r* is also transformed introducing the non-dimensional coordinate $\phi \in [0,1]$, thus:

$$\xi^{I} = \frac{z}{H(\mathbf{r},t)} \quad 0 < z < H(r,t), \; \xi^{II} = \frac{z - H(r,t)}{L - H(r,t)} \quad H(r,t) < z < L, \; \phi = \frac{r}{R_{gl}} \quad 0 < r < R_{gl} \tag{6}$$

Figure 1 shows, on the right hand side, the geometry of the vial in the new non-dimensional coordinates system. In order to solve the problem each function of (*z*, *r*, *t*), namely the temperatures, the pressures, etc., and its derivatives have to be transformed accordingly to the change of coordinates defined by the eqs. (6).
The numerical solution of the problem has been carried out by discretising the spatial domains of the system, thus transforming the PDE problem into an ODE system, and the spectral (or pseudo-spectral) orthogonal collocations method has been adopted in order to find the solution in the nodes of the discretised domain.
The proposed procedure can be applied until the axial flux at the interface is higher than the radial one, that is until the interface profile is described by a monotone function. If radial flux prevails, than exotic geometries may arise, consisting in the formation of a "ball" of frozen product. This event will be discussed in the next section, and finally an alternative double-immobilization procedure will be proposed in the Appendix.

4. RESULTS AND DISCUSSION

The model has been tested with some cases taken from the Literature concerning the freeze-drying of skim milk, which has been often used as a test product in literature, since it can be regarded as a complex pharmaceutical, in the sense that it contains enzymes and proteins (Liapis and Bruttini, 1994).
In Figure 2 the time evolution of the moving interface position (left hand side) and of the ice core temperature (right hand side) are compared with the experimental results obtained from the data published by Wolff and Gibert (1989) for a vial filled with 7 mm of product. The conditions and the parameters for skim milk used in the simulations are taken from Millman et al. (1985). Concerning the core temperature, the comparison has been made considering the mean value of T_{II} along *z* in correspondence of the axis of the vial. It can be seen that the model provides good predictions of the displacement of the moving interface. The simulated frozen core temperature is also in acceptable agreement with the experimental data, with error in the range of 2°C. The slight initial decrease of the predicted temperature is due to the energy absorbed by the sublimation process which is not compensated enough by the heat input provided by the shelf in the very beginning of the primary drying.
It appears from published works concerning multidimensional modelling of freeze-drying, that in typical lyophilization conditions radial gradients are usually small, even when radiation from the environment is taken into account. This is in agreement with the results given by Pikal (1985), where it was found with a series of experiments that the temperature at the bottom centre of the vial was equal to the temperature of the bottom edge, within the uncertainty in temperature measurement (0.5 °C). This aspects have been also confirmed by our simulations and some results are given in the following.

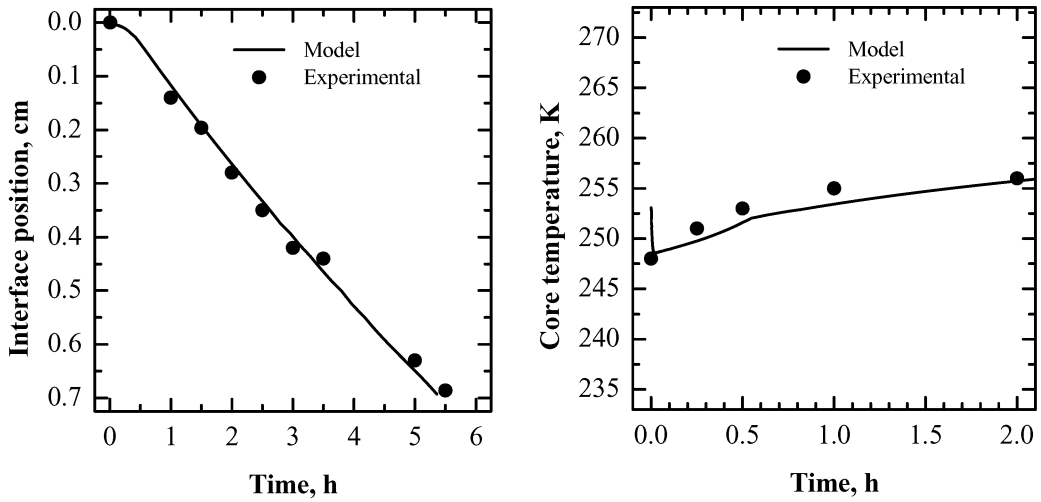

Fig. 2: Comparison between model simulations and experimental results by Wolff and Gibert (1989). Left hand side: interface position. Right hand side: frozen core temperature.

Operating conditions are the same used by Sheehan and Liapis (1998), main parameters are reported in Table 3. During the first 3 h of primary drying, shelf temperature is raised from the initial value of 233.15 K up to 263.15 K. Radiative conditions representative of a real situation, in which the vials are arranged in square arrays and the walls of the chamber have a mean temperature of 273.15 K, have been considered.

Table 3: Values of the variables and parameters adopted in the simulations of Fig. 3 and Fig. 4.

Parameter	Value	Unit	Parameter	Value	Unit
p_{in}	4	Pa	L	$2 \cdot 10^{-2}$	m
p_w	1.07	Pa	R_{gl}	$5 \cdot 10^{-3}$	m
F_{side}	0.795		δ_b	$1 \cdot 10^{-3}$	m
F_{top}	0.75		δ_s	$1 \cdot 10^{-3}$	m

The temperature that two thermocouples placed at $z/L = 0.5$ would read, one in correspondence of the vial centre ($r/R_{gl} = 0$) and the other at the vial edge ($r/R_{gl} = 1$), has been determined taking into account radiation from the chamber. In Figure 3, on the left hand side, the simulated temperatures and the radial ΔT calculated as $T\big|_{r/R_{gl}=1} - T\big|_{r/R_{gl}=0}$ are shown. Up to $t = 8.7$ h the thermocouples would measure the temperature of the frozen mass and the observed radial ΔT is almost zero. Afterwards, in correspondence of the passage of the moving interface from the axial position $z/L = 0.5$, the simulated temperatures become representative of the dried mass. A change in the slope of the temperature profile is thus observed since the thermal conductivity of the frozen and dried layer are different. Of course this change does not occur in the same instant both at $r/R_{gl} = 0$ and $r/R_{gl} = 1$, since the interface is slightly curved and the passage of the interface at $z/L = 0.5$ first is observed at the vial edge, after 8.7 h, and it is completed at the vial centre at $t = 8.8$ h. After this point a radial ΔT is observed, which is always smaller than 1°C and continuously decreases up to the end of the primary drying, while the moving front displaces down to the vial bottom. On the right hand side, the shape of the moving interface $H(r, t)$ is given at three different times. The model correctly predicts a parabolic shape which is curved downward. However, the interface has always got a very small curvature: it can be calculated that the contact angle between the interface and the vial edge is of the order of 0.5 degrees, and the difference between the front position at the vial centre

and at the vial side, given by $H(r,t)\big|_{r=0} - H(r,t)\big|_{r=R_{gl}}$, is always less than 1% of the total height of the product.

It emerges from the previous analysis that the reduction of the primary drying time is the major effect caused by taking into account radiation from the environment. The observed radial gradients have been found to be small; thus, it appears reasonable the simplification of accounting for a symmetric contribution of radiation from the vial side. Furthermore, under the condition of small radial effects, a mono-dimensional model becomes a suitable alternative to the bi-dimensional one.

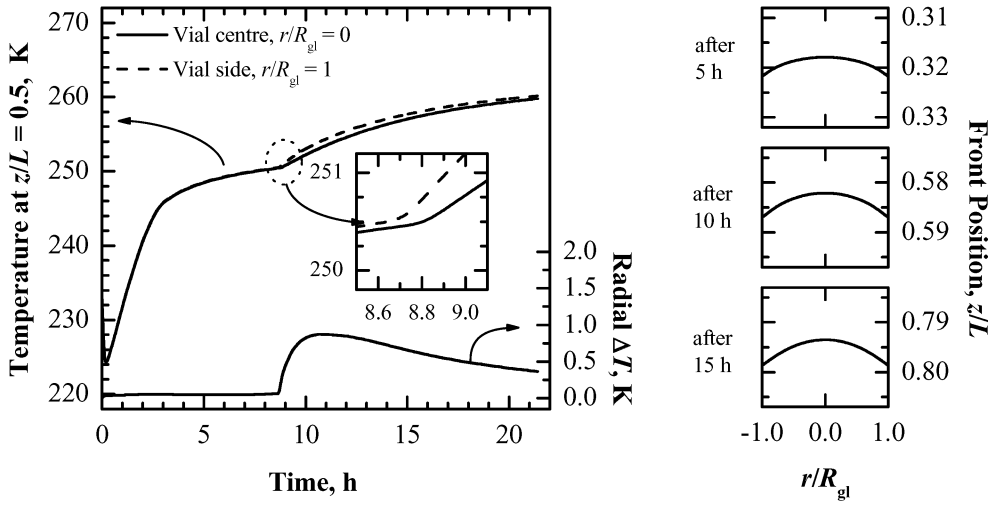

Fig. 3: L.h.s.: radial temperature gradient (right y-axis) and product temperature (left y-axis) taken at axial position z/L = 0.5 and at radial position r/R$_{gl}$ = 0 (vial centre) and r/R$_{gl}$ = 1 (vial edge). R.h.s.: shape of the moving interface taken at t = 5, 10, 15 h during primary drying.

In the following, a comparison between the bi-dimensional (2D) and mono-dimensional (1D) model predictions is presented. Figure 4 (bottom-left hand side) shows three temperature profiles. The continuous curve and the dashed curve are the same given in Figure 3 concerning the bidimensional case, and represent the temperatures that would be measured by two thermocouples placed in correspondence of $z/L = 0.5$, at the vial centre and edge. The dotted curve gives the temperature provided by the monodimensional model, taken at the same axial position. When the moving front arrives at $z/L = 0.5$, corresponding to $t = 8.7$ h, the 2D model starts predicting a small radial ΔT. In the small box plotted in Figure 4 it can be seen that the temperature predicted for the dried layer in the 1D case is comprised between the two values obtained at the extreme radial positions. This is best shown on the right hand side, where the temperature difference $T_{1D} - T_{2D}$ has been plotted, denoting with T_{1D} and T_{2D} respectively the temperature provided in the 1D and 2D case. It can be observed that when the temperature of the frozen mass is measured ($t < 8.7$ h), T_{1D} is slightly higher than T_{2D}, both at $r/R_{gl} = 0$ and $r/R_{gl} = 1$. After 8.7 h the difference in the dried layer is larger, but always lower than 1 K, the maximum observed radial ΔT.
Figure 4 (top-left hand side) depicts the evolution of the position of the moving interface, and full agreement is found between the two models. Even if the scale of the figure does not allow to appreciate the difference between the planar 1D front position and the curved 2D interface, it can be observed that the position of the planar interface is always slightly overestimated since in the frozen layer the temperature predicted by the 1D model is little higher than the 2D. However, it can be calculated that the 2D shape can be approximated by the planar 1D interface, within an error of the order of 1-1.5% of the total height of the sample. Thus, the results given in Figure 4 confirm that the mono-dimensional model can be adopted as a suitable alternative to the 2D approach.

More complex to describe is the case when an ice core is formed, instead of a simple curved surface, that can be described by a monotone function; this can happen when radial effects are very strong. The mechanism of formation of this ice core can be also enhanced by the presence of non-uniformities in the physical properties of the product, and in practice it constitutes an undesirable event. Even if the model equations can theoretically predict this uncommon behaviour, care must be paid in posing the problem in the correct mathematical form. In fact, the previously described approach based on the introduction of the function $H(r, t)$ fails to describe the pathological ice core formation. A double axial-radial immobilisation procedure can be proposed in this case, as described in the appendix, where also a schematic of the process of formation of the ice core is depicted in Figure A1.

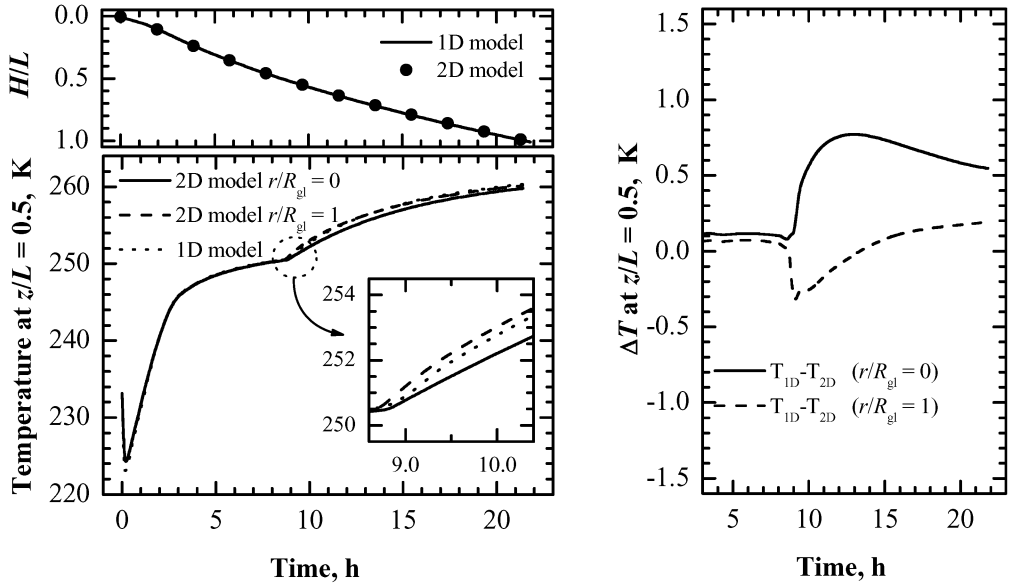

Fig. 4: Comparison between 1D and 2D model. L.h.s.: time evolution of the dimensionless position of the moving interface H/L, and product temperature at axial position z/L = 0.5. For the 2D model temperatures are taken at radial position $r/R_{gl} = 0$ (vial centre) and $r/R_{gl} = 1$ (vial edge). R.h.s.: difference between the temperature predicted by the two models.

5. CONCLUSIONS

The effect of radiating heat on primary drying has been discussed: it causes the sublimating interface to be curved, but this effect is generally limited, and a mono-dimensional model can describe the phenomena with sufficient accuracy. Nevertheless, it is possible that in some particular cases pronounced radial effects might be obtained, if the energy supplied to the vial has a very strong component in the radial direction compared to the axial one, what is normally not observed in vial lyophilization. Furthermore, this is regarded as an unwanted situation, since it can lead to non-uniformities in the product and to the formation of an "ice core" inside the porous matrix during primary drying. These aspects will be object of a future work, but a mathematical procedure has been proposed for this case.

Acknowledgements. The contribution of Davide Fissore to the preparation of the manuscript is greatly acknowledged.

6. REFERENCES

Barresi A.A., Fissore D. and Marchisio D.L., 2010, Process Analytical Technology in industrial freeze-drying, in: "Freeze-Drying/Lyophilization of Pharmaceuticals and Biological Products, 3rd rev. Edition" (L. Rey and J. C. May, Eds.), Chap. 20. Informa Healthcare, New York, pp. 463-496.

Fissore D., Pisano R. and Barresi A.A., 2010, A rational approach to process transfer and scale up in freeze-drying of pharmaceutical products. Proceedings of 17th International Drying Symposium (IDS2010) (E. Tsotsas, T. Metzger, M. Peglow, Eds.), October 3-6, Magdeburg, Germany, Vol. C, pp. 2178-2185.

Giordano A., Barresi A.A. and Fissore D., 2011, On the use of mathematical models to build the design space for the primary drying phase of a pharmaceutical lyophilization process. J. Pharm. Sci. 100, 311-324.

Kast W. and Hohenthanner C.R., 2000, Mass transfer within the gas phase of porous media, Int. J. Heat. Mass. Transf. 43, 807-823.

Liapis A.I. and Bruttini R., 1994, A theory for the primary and secondary drying stages of the freeze-drying of pharmaceutical crystalline and amorphous solutes: A comparison between experimental data and theory, Separ. Technol. 4, 144-155.

Liapis A.I. and Bruttini R., 1995, Freeze-drying of pharmaceutical crystalline and amorphous solutes in vials: Dynamic multi-dimensional models of the primary and secondary drying stages and qualitative features of the moving interface, Drying Technol. 13, 43-72.

Liapis A.I., Pikal M.J. and Bruttini R., 1996, Research and development needs and opportunities in freeze-drying, Drying Technol. 14, 1265-1300.

Lienhard J.H. IV and Lienhard J.H V, 2004, A Heat transfer Textbook. Phlogiston Press, Cambridge.

Lombraña J.I, De Elvira C. and Villaran M.C., 1997, Analysis of operating strategies in the production of special foods in vial by freeze-drying, Int. J. Food Sci. Tech. 32, 107-115.

Mascarenhas W.J., Akay H.U. and Pikal M.J., 1997, A computational model for finite element analysis of the freeze-drying process, Comput. Method Appl. M. 148, 105-124.

Mason E.A., Malinauskas A.P. and Evans, R. B. III, 1967, Flow and diffusion of gases in porous media, J. Chem. Phys. 46, 3199-3216.

Millman M.J., Liapis A.I. and Marchello J.M., 1985, An analysis of the lyophilisation process using a sorption sublimation model and various operational policies, AIChE J. 31(10), 1594-1604.

Pikal M.J., 1985, Use of laboratory data in freeze-drying process design: heat and mass transfer coefficients and the computer simulation of freeze-drying, J. Parenter. Sci. Technol. 39, 115–139.

Pisano R., Fissore D., Velardi S.A. and Barresi A.A, 2010, In-line optimization and control of an industrial freeze-drying process for pharmaceuticals, J. Pharm. Sci. 99, 4691-4709.

Rasetto V., Marchisio D.L., Fissore D. and Barresi A.A., 2010, On the use of a dual-scale model to improve understanding of a pharmaceutical freeze-drying process, J. Pharm. Sci. 99, 4337-4350.

Sadikoglu H. and Liapis A.I., 1997, Mathematical modeling of the primary and secondary stages of bulk solution freeze-drying in trays: parameter estimation and model discrimination by comparison of theoretical results with experimental data, Drying Technol. 13, 43-72.

Sheehan P. and Liapis A.I., 1998, Modeling of the primary and secondary drying stages of the freeze-drying of pharmaceutical product in vials: numerical results obtained from the solution of a dynamic and spatially multi-dimensional lyophilisation model for different operational policies, Biotechnol. Bioeng. 60, 712-728.

Tang M.M., Liapis A.I. and Marchello J.M., 1986, A multi-dimensional model describing the lyophilization of a pharmaceutical product in a vial, Proceedings of the 5th International Drying Symposium (A.S. Mujumadar, Ed.). Hemisphere Publishing Company, New York, vol. 1, pp. 55-65.

Velardi S.A. and Barresi A.A., 2008, Development of simplified models for the freeze-drying process and investigation of the optimal operating conditions, Chem. Eng. Res. Des. 86, 9-22.

Velardi S.A., Hammouri H. and Barresi A.A., 2009, In-line monitoring of the primary drying phase of the freeze-drying process in vial by means of a Kalman filter based observer, Chem. Eng. Res. Des. 87, 1409-1419.

Velardi S.A, Hammouri H. and Barresi A.A., 2010, Development of a High Gain observer for in-line monitoring of sublimation in vial freeze-drying, Drying Technol. 28, 256-268.
Wolff E. and Gibert H., 1989, Vacuum freeze-drying kinetics and modelling of a liquid in a vial, Chem. Eng. Proc. 25, 153-158.

APPENDIX

Depending on the relative weight of the heat contribution from the vial sides and from the top and bottom of the vial, the radial heat flux at the interface can be locally higher than the axial flux leading to the formation of a "ball" of frozen product. A schematic of the process of formation of the ice core is depicted in Figure A1.

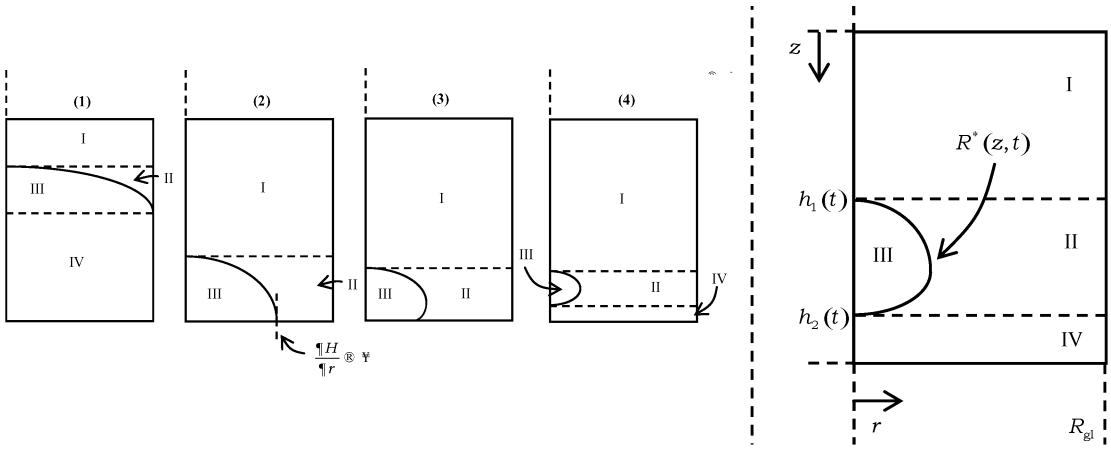

Fig. A1: Left hand side: Ice core formation. Right hand side: the moving interface described in terms of the function $R^*(z, t)$.

At a certain time during primary drying, corresponding to the situation (2), the moving interface becomes perpendicular to the vial bottom. Afterwards, cases (3) and (4), the profile given by the function $H(r, t)$ is no longer monotonous and it occurs that two distinct values of H could be possible in correspondence of the same radial position. It follows that the procedure of immobilisation of the spatial grid described in section 3 can not be applied, since $H(r, t)$ is not a bijective function. In this case it is more useful to express the position of the moving interface with the inverse function of H, denoted as $R^*(z, t)$, which is a bijective function; thus, whatever the position of the moving front, only one value of R^* is possible for a given axial position.
If the upper and lower axial positions of the interface are described by the functions $h_1(t)$ and $h_2(t)$, four mathematical domains can be individuated. The "double axial-radial immobilisation" of the moving front introduces 4 non-dimensional axial and radial coordinates, denoted with $\xi^i(z,t)$ and $\phi^i\left(\xi^i(z,t),r,t\right)$ respectively, one for each domain. Table A1 shows the spatial limits of the four domains, the expressions of the non-dimensional spatial coordinates and of their derivatives. It can be seen that with the previous substitutions the domain of variability of each non-dimensional coordinate is fixed, so that ξ^j and $\phi^j \in [0,1]$ with $j = \mathrm{I},\ldots,\mathrm{IV}$. In order to solve the problem, each function $f(z, r, t)$, namely T_I, T_II, ρ_w, ρ_in, R^*, $\mathbf{N_w}$, $\mathbf{N_{in}}$, and its derivatives have to be transformed accordingly to the change of the coordinates system. The transformed expressions of $f(z, r, t)$ and of the derivatives in the non-dimensional space are given in Table A2. For instance, the mass balance equation for the inert component in the domain III can be written as:

$$\varepsilon_p \frac{\partial \rho_{\text{in}}}{\partial t} = -\left(\frac{\partial N_{\text{in},\xi}}{\partial \xi} + \frac{\partial N_{\text{in},\phi}}{\partial \phi} \frac{1-\phi}{R_{\text{gl}} - R^*} \dot{R}^*_\xi \right) \frac{\xi \dot{h}_{2t} + (1-\xi)\dot{h}_{1t}}{h_2 - h_1} - \left(\frac{\partial N_{\text{in},\phi}}{\partial \phi} + \frac{N_{\text{in},\phi}}{\phi\left(R_{\text{gl}} - R^*\right) + R^*} \right) \frac{1}{R_{\text{gl}} - R^*} +$$
$$-\varepsilon_p \frac{\partial \rho_{\text{in}}}{\partial \xi} \frac{\xi \dot{h}_{2t} + (1-\xi)\dot{h}_{1t}}{h_2 - h_1} - \varepsilon_p \frac{\partial \rho_{\text{in}}}{\partial \phi} \frac{1-\phi}{R_{\text{gl}} - R^*} \left(\dot{R}^*_t + \dot{R}^*_\xi \frac{\xi \dot{h}_{2t} + (1-\xi)\dot{h}_{1t}}{h_2 - h_1} \right) \tag{A1}$$

with $\phi = \phi^{\text{III}}$, $\xi = \xi^{\text{III}}$, $\rho_{\text{in}} = \rho_{\text{in}}^{\text{III}}\left(\xi^{\text{III}}, t, \phi^{\text{III}}\right)$, $N_{\text{in},\xi} = N_{\text{in},\xi}^{\text{III}}\left(\xi^{\text{III}}, t, \phi^{\text{III}}\right)$, $N_{\text{in},\phi} = N_{\text{in},\phi}^{\text{III}}\left(\xi^{\text{III}}, t, \phi^{\text{III}}\right)$

Table A1: Expressions of the non-dimensional axial and radial coordinates in the four domains *j* = I, .., IV.

Domain	**I**	**II**	**III**	**IV**
Limits	$0 < z < h_1$ $0 < r < R_{\text{gl}}$	$h_1 < z < h_2$ $R^* < r < R_{\text{gl}}$	$h_1 < z < h_2$ $0 < r < R^*$	$h_2 < z < L$ $0 < r < R_{\text{gl}}$
Non-dimensional axial coordinate, ξ^i	$\frac{z}{h_1}$	$\frac{z - h_1}{h_2 - h_1}$	$\frac{z - h_1}{h_2 - h_1}$	$\frac{z - h_2}{L - h_2}$
Derivatives along z, $\dot{\xi}^i_z$	$\frac{1}{h_1}$	$\frac{1}{h_2 - h_1}$	$\frac{1}{h_2 - h_1}$	$\frac{1}{L - h_2}$
Derivatives along t, $\dot{\xi}^i_t$	$-\frac{\xi^i \dot{h}^i_{1t}}{h_1}$	$\frac{\xi^i \dot{h}^i_{2t} + \left(1-\xi^i\right)\dot{h}^i_{1t}}{h_2 - h_1}$	$\frac{\xi^i \dot{h}^i_{2t} + \left(1-\xi^i\right)\dot{h}^i_{1t}}{h_2 - h_1}$	$-\frac{\left(1-\xi^i\right)\dot{h}^i_{2t}}{L - h_2}$
Non-dimensional radial coordinate, ϕ^i	$\frac{r}{R_{\text{gl}}}$	$\frac{r - R^*}{R_{\text{gl}} - R^*}$	$\frac{r}{R^*}$	$\frac{r}{R_{\text{gl}}}$
Derivatives along *z*, $\dot{\phi}^i_{\xi^i}$	0	$\frac{1-\phi^i}{R_{\text{gl}} - R^*} \dot{R}^*_\xi$	$-\frac{\phi^i}{R^*} \dot{R}^*_\xi$	0
Derivatives along *t*, $\dot{\phi}^i_t$	0	$\frac{1-\phi^i}{R_{\text{gl}} - R^*} \dot{R}^*_t$	$-\frac{\phi^i}{R^*} \dot{R}^*_t$	0
Derivatives along *r*, $\dot{\phi}^i_r$	$\frac{1}{R_{\text{gl}}}$	$\frac{1}{R_{\text{gl}} - R^*}$	$\frac{1}{R^*}$	$\frac{1}{R_{\text{gl}}}$

Table A2: Expression of the generic function $f(z, r, t)$ and its derivatives in the non-dimensional space.

	Original coordinates	**Non-dimensional coordinates**
Variables	r, z, t	ϕ^i, ξ^i, t
Function	$f(r,z,t)$	$f^i\left(\phi^i, \xi^i, t\right)$
Derivatives	$\dot{f}^i_r(r,z,t)$	$\dot{f}^i_\phi \dot{\phi}^i_r$
	$\dot{f}^i_z(z,t,r)$	$\left(\dot{f}^i_\xi + \dot{f}^i_\phi \dot{\phi}^i_\xi\right)\dot{\xi}^i_z$
	$\dot{f}^i_t(r,z,t)$	$\dot{f}^i_t + \dot{f}^i_\xi \dot{\xi}^i_t + f^i_\phi\left(\phi^i_t + \phi^i_\xi \xi^i_t\right)$
	$\ddot{f}^i_{rr}(r,z,t)$	$\ddot{f}^i_{\phi\phi}\left(\dot{\phi}^i_r\right)^2$
	$\ddot{f}^i_{zz}(r,z,t)$	$\left[\ddot{f}^i_{\xi\xi} + 2\ddot{f}^i_{\phi\xi}\dot{\phi}^i_\xi + \dot{f}^i_\phi \ddot{\phi}_{\xi\xi} + \ddot{f}^i_{\phi\phi}\left(\dot{\phi}^i_\xi\right)^2\right]\left(\dot{\xi}^i_z\right)^2$